

An ODE Model of A Breast Cancer Tumor: HER2+
MTSU MATHEMATICAL SCIENCES DEPARTMENT

A Thesis

Presented to the Faculty of the Department of Mathematical Sciences
Middle Tennessee State University

In Partial Fulfillment
of the Requirements for the Degree
Master of Science in Mathematical Sciences

by

Greg Owanga

03/27/2023

Thesis Committee:

Member 1, Chair Dr. Rachel Natalie Leander

Member 2, Dr. Wandi Ding

Member 3, Dr. Yixiang Wu

Member 4, Dr. Chris Stephens

Member 5, Dr. James Hart

Member 6, Dr. David. E Nelson

APPROVAL

This is to certify that the Graduate Committee of

Greg Owanga

met on the

7th day of April, 2023.

The committee read and examined his thesis, supervised his defense of it in an oral examination, and decided to recommend that his study should be submitted to the Graduate Council, in partial fulfillment of the requirements for the degree of Master of Science in Mathematics.

Dr. Rachel Leander
Chair, Graduate Committee

Dr. Wandi Ding

Dr. Yixiang Wu

Dr. David. E Nelson

Dr. James Hart
Graduate Coordinator,
Department of Mathematical Sciences

Dr. Chris Stephens
Chair,
Department of Mathematical Sciences

Signed on behalf of
the Graduate Council

Dr. David Butler
Dean,
School of Graduate Studies

DEDICATION

To my wonderful mom Françoise Ghéongault Mokoukou
and my sisters Shanon, Océane, Belle Jasmine, Orchidée, and Gloire.

ACKNOWLEDGMENTS

I thank my wonderful thesis mentor, Dr. Rachel Leander, for helping me to complete this work and believing in me. I would also like to thank Dr. Víctor M. Pérez-García for providing the tumor volume data for model validation.

ABSTRACT

We are developing an ODE model of a human epidermal growth factor receptor 2-positive (HER2+) breast cancer tumor that accounts, in a simplified way, for the tumor structure and interaction with the immune system. Mounting empirical research suggests that the tumor stroma or tumor interface zone is a critical determinate of the propensity of the cancer to invade and/or metastasize. Likewise, there is increasing interest in cancer therapies that encourage the immune system to target and destroy cancer cells. We describe tumor growth while accounting for the interface zone and the interaction between the tumor and natural killer cells (NK cells). Interactions between HER2+ breast cancer tumor cells and NK cells can be influenced by the antibody drug trastuzumab, and we use our model to investigate tumor growth (i) in isolation, and (ii) in the presence of NK cells and trastuzumab. Model predictions are compared to empirical data on tumor growth. We found that increasing the cytotoxicity of patrolling NK cells may be insufficient for the control of highly aggressive tumors (those with very fast proliferation or high density). However, if healthy tissue has high levels of patrolling cytotoxic NK cells, then the tumor cannot exist.

Contents

LIST OF TABLES	viii
LIST OF FIGURES	ix
CHAPTER 1: INTRODUCTION	1
CHAPTER 2: A SIMPLE MODEL OF TUMOR GROWTH	5
2.1 Model derivation	5
2.2 Characterization of tumor growth in terms of R	10
2.3 Instantaneous Doubling Time for Small and Large Tumors	13
CHAPTER 3: NATURAL KILLER CELLS IN BREAST CANCER, BACKGROUND	15
3.1 NK cell range/specificity	16
3.2 NK cell type, activation, and exhaustion/subversion by the tumor . .	17
3.3 NK cell recruitment	18
CHAPTER 4: A MODEL OF NK CELLS WITHIN A TUMOR ...	19
4.1 Modeling NK Cells Killing and Activation	19
4.2 Recruitment of NK cells	21
4.3 Modeling NK population expansion through immune system activation	23
4.4 Tumor-induced exhaustion of active cytotoxic NK cells	24
4.5 Differential equations for NK cells in the presence of immune system activation	25
CHAPTER 5: A MODEL OF TUMOR GROWTH WITH DRUG-INDUCED IMMUNE SYSTEM ACTIVATION	27
CHAPTER 6: QUALITATIVE ANALYSIS OF THE MODEL OF TUMOR GROWTH WITH IMMUNE SYSTEM ACTIVATION.	30
CHAPTER 7: NUMERICAL SIMULATIONS	32
CHAPTER 8: DISCUSSION AND FUTURE DIRECTIONS	37
CHAPTER 9: CONCLUSION	39

BIBLIOGRAPHY 40

List of Tables

1	Model Parameters	36
2	Other Values from the Literature	36

List of Figures

1	Comparison of Biological and Mathematical Tumor Models: Left: A biological model of a tumor including a central tumor core and interface zone. Right: A mathematical model of a tumor including a central core and peripheral growth region.	6
2	Schematic for NK cell dynamics in the presence of tumor-induced immune system activation. 1. Cytotoxic NK cells are recruited to the tissue from the blood. 2. In the presence of trastuzumab, tumor cells activate NK cells. 3. Tumor-activated NK cells kill tumor cells and 4. recruit additional active, cytotoxic NK cells to the tumor site. 5. Newly recruited NK cells contribute to tumor cell killing. 6. In the presence of tumor cells, tumor-activated cytotoxic NK cells gradually become exhausted. Legend: NK^c : cytotoxic NK cells, NK^* : active, NK_p^* : newly recruited, cytotoxic NK cells, NK_e : exhausted NK cells, active, cytotoxic NK cells, T_G : tumor cells in the growth region.	26
3	Hamartoma Volume Patient 1.	33
4	Hamartoma Volume Patient 2.	34
5	Hamartoma Volume Patient 3.	34
6	Hamartoma Volume Patient 4.	35
7	Hamartoma Volume Patient 5.	35
8	Hamartoma Volume Patient 6.	36

CHAPTER 1

INTRODUCTION

Cancer is a leading causes of death worldwide [44]. In the US alone, 602,350 people died of cancer in 2020 [22], and approximately 1.9 million people were diagnosed in 2022 [31]. As a result, billions of dollars are spent on cancer research every year. Indeed, the National Institute of Cancer offered \$6.4 billion of cancer research funding in 2020 [32]. In 2022, breast cancer became the most diagnosed cancer worldwide [64, 44], with approximately 2.3 million new cases recorded in that year alone [64, 44]. At the molecular level, breast cancer is generally classified as one of four types according to the expression of hormone receptors (HR) (i.e. estrogen receptor or progesterone receptor[12]) and human epidermal growth factor receptor 2: HR+/HER2-; HR+/HER2+; HR-/HER2+; and HR-/HER2- [47]. The four-year survival rates for HR+/HER2-, HR+/HER2+, HR-/HER2+, and HR-/HER2- are 93.5%, 90.3%, 82.7%, and 77.0%, respectively [47].

This work concerns the mathematical modeling of breast cancer tumor growth and therapeutic intervention. Our model of therapy is specific to HER2+ cancers. Approximately 15 to 20% of breast cancers are HER2+ [53]. These cancers are frequently treated with the antibody drug trastuzumab which can be used in combination with additional drugs and chemotherapy [47, 27, 55, 58, 6, 2]. Trastuzumab works by binding to receptors on the cell surface[21, 66, 58], thereby reducing cancer cell proliferation and exposing cancer cells to Natural Killer (NK) cell- mediated cytotoxicity [58, 55, 35, 68].

There exists a large body of research on mathematical modeling of tumors using diverse techniques including ordinary differential equations (ODEs) [61, 3, 16, 17, 36, 60, 43, 34, 13, 51, 45], stochastic differential equations [14, 39], and partial differential equations (PDEs) [67, 15, 30, 7, 63, 62]. See [65] for a review of mathematical contributions to solid tumor research. We briefly summarize some works of note which are related to our work in that they consider the impact of therapy, the immune system, and/or spatial structure on cancer growth. ODEs are often used to model the impact of the immune system and immunotherapy on cancer growth. In [17], de Pillis et al. developed an ODE model to describe the role of NK cells and CD8⁺ T cells in the tumor-immune response. This model considered three types of

cells: tumor cells, NK cells, and $CD8^+$ T cells. The model described logistic cancer cell proliferation, killing of cancer cells by cytotoxic NK and $CD8^+$ T cells, tumor-induced enhancement of immune cell cytotoxicity, NK cell-mediated recruitment of $CD8^+$ T cells, and immune cell exhaustion. The two types of immune cells present were assumed to exhibit different functional forms for tumor cell lysis, and this difference was found to be critical for cancer control efficacy [17]. In other work [34], Kronik et al. used a system of DEs to predict the outcome of immunotherapy applied to prostate cancer. The model, which included cancer cells, cancer vaccine, dendritic cells, and immune effector cells, was found to have significant predictive power. Similarly, Ouerdani et al. [45] used ODEs to develop a model for the growth of benign tumors in patients with neurofibromatosis type 2. The model, which was able to describe and predict tumor volume growth with and without treatment, included a nonlinear growth function which approximated exponential growth for small tumors and linear growth for large tumors. In [17, 34], cancer burden was measured by cancer cell number or density, both of which are directly proportional to tumor volume. However, in some works, cancer burden is measured instead by tumor radius or diameter [51, 13]. The model measure of tumor burden is generally determined by the empirical data to which the model will be compared. Irrespective of the type of tumor burden measurement, when modeling with ODEs, the functional form for tumor growth is typically selected to fit empirical data. Hence ODE models of tumor growth tend to be phenomenological in nature. More mechanistic models of tumor growth are generally based on systems of PDEs [15, 30, 7, 67, 63, 62]. PDEs are a natural choice for describing the tumor geometry and its impact on the spatial distribution of nutrients, inhibitors, and mechanical forces, which combine to determine tumor growth. For example, a PDE model for drug transport within a breast cancer tumor was developed in [36]. The model was used to study how quantities important for therapy outcome, including the maximal drug concentration and time-averaged drug concentration, vary with the tumor radius and distance from the tumor boundary. Other authors have described tumor growth as a free boundary problem [67, 15, 24, 7]. In these models, the tumor is usually supposed to be spherically symmetrical to improve mathematical tractability, but see [29] for an exception. In [24] a model for tumor growth with angiogenesis was developed and analyzed. The model predicted that when the tumor proliferation rate is small, the

tumor exhibits a stable steady state, while tumors exhibiting fast proliferation can grow indefinitely. In [15] a model of tumor growth with quiescent and proliferating cells is considered and it is shown that, under certain restrictions, this tumor model exhibits an asymptotically stable steady state. In [67] a model of tumor growth in the presence of nutrients and a therapeutic inhibitor was considered. Under some assumptions, the model tumor radius is shown to be bounded, and the tumor may persist or vanish depending on the concentration of the inhibitor. Finally, in [63] a spatial model of tumor growth which accounts for the impact of mechanical stress was developed, parameterized, and validated with patient data.

In this work, we construct a spacial model of tumor growth using ODEs to evaluate the impact of immune system interactions with the tumor in space. Indeed, as described in section 3.1, geometry and spatial constraints can influence tumor-immune system interactions.

In this work, we use ODEs to construct a spatial model of tumor growth for the purpose of evaluating the interactions between the tumor and immune system in space. Indeed, as discussed in section 3.1, geometry and spatial constraints can influence tumor/immune system interactions. We begin with a simple model of tumor growth accounting for the spatial structure of the tumor. The model describes a two-part tumor consisting of a proliferative peripheral growth region and central tumor core. The tumor core represents a relatively quiescent region that has reached confluent cell density. The peripheral growth region represents the tumor interface zone or stroma [40]. It should be noted that our simple model does not include necrotic cancer tissue. After analyzing this simple model, we incorporate immune system activation into the model to consider the impact of trastuzumab treatment on tumor growth.

To the best of our knowledge, this work is unique in that it uses ordinary differential equations to model structured tumor growth with immune system activation. This approach results in models that more amenable to mathematical analysis and numerical simulations than the systems of partial differential equations and free boundary problems typically used to study spatial tumor growth. Hence, this work has the potential to provide additional insights into the fundamental process of tumor growth.

This manuscript is organized as follows. In section 2, we describe our model of

tumor growth without drug-induced immune system and characterize the growth of large and small tumors. In section 3, we give a general background on NK cells (i.e., range, activation, exhaustion, and recruitment of NK cells). In section 4, we describe our mathematical model of NK cells. In section 5, we add NK cell killing into our tumor model. In section 6, we do a qualitative analysis of the model of tumor growth with drug-induced immune system activation. In section 7, we use numerical simulation to test the model's ability to describe tumor growth data. In section 8, we give a general discussion and open the door to future work. Finally, in section 9, we provide a general conclusion of our manuscript.

CHAPTER 2

A SIMPLE MODEL OF TUMOR GROWTH

2.1 Model derivation

In this paper, we suppose the tumor has a spherical form. The tumor has two components: a central core and a peripheral region where tumor growth and invasion occurs. We refer to the former as the core and the latter as the growth region. We let V_T denote the volume of the tumor, V_c denote the volume of the core, and V_G denote the volume of the growth region. The radius of the tumor is denoted by $R(t)$, and the width of the growth region is denoted by d . One assumption of the model is that the width of the growth region is determined by processes, such as diffusion of nutrients, that occur at the cellular and subcellular level, and hence is constant/independent of the tumor's size (*i.e.* d is constant). See figure 1 for a visual comparison of a real-world and model tumor. Let the number of tumor cells in the growth region to be $T_G(t)$, and the number of tumor cells in the core region be $T_C(t)$. The density of cells in the growth region is D_G , and the density of cells in the core is D_C . We assume that the density of cells in the growth region is less than the density of cells in the core region (*i.e.* $D_G < D_C$), and that both densities are constant. This simplification is motivated by the fact that different cell types are characterized by a steady-state density [42]. Hence, the assumption of constant density in each compartment can be viewed as a quasi-steady state assumption. In this model, we assume additionally that net population growth is the result of proliferation in the growth region. This does not necessarily imply that cells in the core are unable to die or proliferate, only that proliferation and death are exactly balanced in the core region. Next we derive differential equations to describe tumor growth under these assumptions.

The radius of the tumor core is:

$$R_C(t) = R(t) - d. \tag{2.1.1}$$

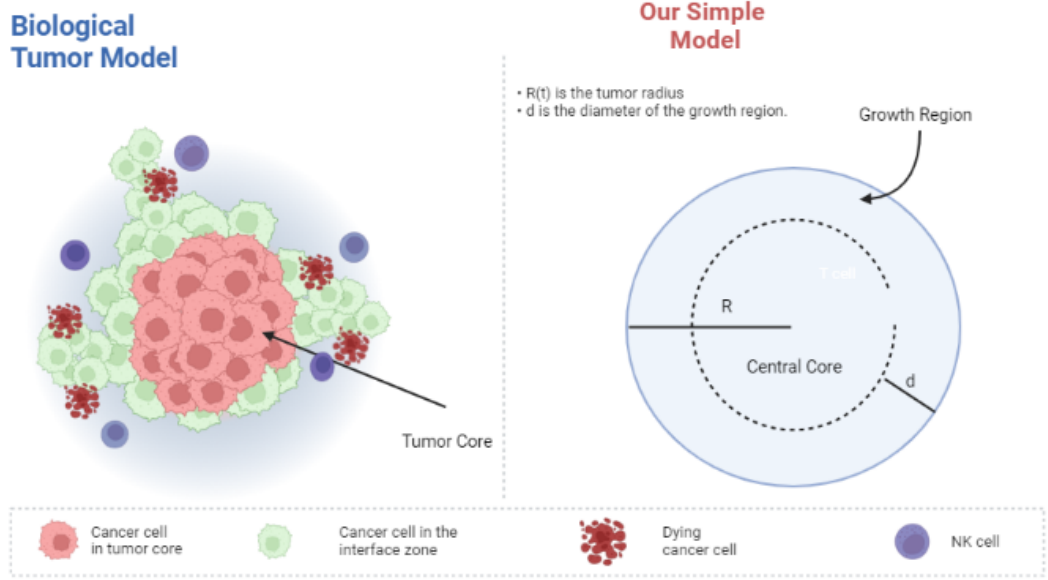


Figure 1: Comparison of Biological and Mathematical Tumor Models: Left: A biological model of a tumor including a central tumor core and interface zone. Right: A mathematical model of a tumor including a central core and peripheral growth region.

The cell number and volume of the growth region are related as:

$$T_G(t) = D_G \cdot V_G(t) \quad (2.1.2)$$

The cell number and volume of the growth region are related as:

$$T_C(t) = D_C \cdot V_C(t) \quad (2.1.3)$$

Meanwhile each region's volume can be computed in terms of the tumor radius.

$$V_C = \begin{cases} \frac{4}{3}\pi(R - d)^3, & R \geq d \\ 0, & R < d \end{cases} \quad (2.1.4)$$

$$V_G = \begin{cases} 4\pi d \left(R^2 - Rd + \frac{1}{3}d^2 \right), & R \geq d \\ \frac{4}{3}\pi R^3, & R < d \end{cases} \quad (2.1.5)$$

Therefore, $\frac{dT_G}{dt}$ can be computed as a function of R : ($R \geq d$)

$$\begin{aligned} \frac{d}{dt}T_G &= D_G \frac{d}{dt}V_G \\ &= 4\pi d D_G \frac{d}{dt} \left(R^2 - Rd + \frac{1}{3}d^2 \right) \\ &= 4\pi d D_G \left(2R \frac{d}{dt}R - d \frac{d}{dt}R \right) \\ &= 4\pi d D_G (2R - d) \frac{dR}{dt}. \end{aligned}$$

In summary,

$$\frac{d}{dt}T_G = \begin{cases} 4\pi d D_G (2R - d) \frac{dR}{dt}, & R \geq d \\ 4\pi D_G R^2 \frac{dR}{dt}, & R < d \end{cases} \quad (2.1.6)$$

Similarly, we express $\frac{dT_C}{dt}$ in terms of R . ($R \geq d$)

$$\begin{aligned} \frac{d}{dt}T_C &= D_C \frac{d}{dt}V_C \\ &= \frac{4}{3}\pi D_C \frac{d}{dt}(R - d)^3 \\ &= 4\pi D_C (R(t) - d)^2 \frac{dR}{dt}. \end{aligned}$$

So,

$$\frac{d}{dt}T_C = \begin{cases} 4\pi D_C (R(t) - d)^2 \frac{dR}{dt}, & R \geq d \\ 0, & R < d \end{cases} \quad (2.1.7)$$

Recall we have assumed population growth is due to proliferation in the growth region. Hence, if cells in the growth region proliferate at the per capita rate μ , we

have:

$$\mu T_G = \begin{cases} \frac{d(T_G + T_C)}{dt}, & R \geq d \\ \frac{dT_G}{dt}, & R < d. \end{cases} \quad (2.1.8)$$

The previous yields a conservation equation for tumor growth ($R \geq d$)

$$\frac{d}{dt}(T_C + T_G) = 4\pi [D_C R^2 - 2d(D_C - D_G)R + d^2(D_C - D_G)] \frac{dR}{dt} = \mu T_G(t) \quad (2.1.9)$$

Substituting

$$T_G(t) = 4\pi d D_G \left[R^2(t) - R(t)d + \frac{1}{3}d^2 \right] \quad (2.1.10)$$

into 2.1.9 we derive a differential equation in R alone: ($R \geq d$)

$$\frac{dR}{dt} = \mu d D_G \frac{R^2(t) - R(t)d + \frac{1}{3}d^2}{D_C R^2(t) - 2d(D_C - D_G)R(t) + d^2(D_C - D_G)}. \quad (2.1.11)$$

Doing the same analysis for $R < d$, we derive a piece-wise differential equation in R

$$\frac{dR}{dt} = \begin{cases} \mu d D_G \frac{R^2(t) - R(t)d + \frac{1}{3}d^2}{D_C R^2(t) - 2d(D_C - D_G)R(t) + d^2(D_C - D_G)}, & R \geq d \\ \frac{1}{3}\mu R, & R < d \end{cases} \quad (2.1.12)$$

Theorem 1 $\frac{dR}{dt}$ is continuously differentiable for all $R \geq 0$

Proof 1 Let consider 2.1.12 and suppose $R \geq d$, we can express the derivative of $\frac{dR}{dt}$ by

$$\frac{d}{dR}(R'(t)) = \mu d D_G \frac{-d(D_C - 2D_G)R^2 + 2d^2(\frac{2}{3}D_C - D_G)R - \frac{1}{3}d^3(D_C - D_G)}{[D_C R^2 - 2d(D_C - D_G)R + d^2(D_C - D_G)]^2} \quad (2.1.13)$$

When $R = d$, we have

$$\left[\frac{d}{dR}(R'(t)) \right]_{R=d} = \frac{1}{3}\mu$$

Hence $\frac{d}{dR}(R'(t))$ is continuous. That ends the proof.

In the next section we will solve 2.1.11. For this, observe 2.1.11 separates as:

$$\frac{D_C R^2 - 2d(D_C - D_G)R + d^2(D_C - D_G)}{R^2 - Rd + \frac{1}{3}d^2} dR = \mu dD_G dt. \quad (2.1.14)$$

2.2 Characterization of tumor growth in terms of R

In this section will solve 2.1.11 and analyze the behavior of the solution radius in order to determine how the model tumor grows.

Theorem 2 *There exists a unique solution of 2.1.11 together with $R(0) = R_0 \geq d$ for $t \geq 0$. Moreover, this solution is strictly monotone increasing, and satisfies:*

$$\lim_{t \rightarrow \infty} R(t) = \infty.$$

Proof 2 *Let $g(r)$ and $f(r)$ be defined by:*

$$f(r) := D_C r^2 - 2d(D_C - D_G)r + d^2(D_C - D_G)$$

and

$$g(r) := r^2 - dr + \frac{1}{3}d^2,$$

so that 2.1.14 can be expressed as

$$\frac{f(R)}{g(R)} dR = \mu dD_G dt.$$

Let Δ_1 be the discriminant of $f(r)$ and Δ_2 be the discriminant of $g(r)$. We see that,

$$\Delta_1 = -4d^2 D_G (D_C - D_G) < 0 \tag{2.2.1}$$

Thus, $f(r) > 0$ for all $r \in \mathbb{R}$. Since, in addition,

$$\Delta_2 = -\frac{1}{3}d^2 < 0, \tag{2.2.2}$$

$g(r) > 0$ for all $r \in \mathbb{R}$.

Thus, $\frac{dR}{dt} = \mu dD_G \frac{g(R)}{f(R)}$ is C^1 , and hence 2.1.11 together with $R(0) = R_0 > d$ exhibits a unique maximal solution.

Moreover, we may solve 2.1.11 to derive an implicit formula for $R(t)$. We have

$$\begin{aligned} \int \mu dD_G dt &= \int \frac{D_C R^2 - 2d(D_C - D_G)R + d^2(D_C - D_G)}{R^2 - dR + \frac{1}{3}d^2} dR \\ &= \int \left[D_C + \frac{dR(2D_G - D_C) + d^2(\frac{4}{3}D_C - D_G)}{R^2 - dR + \frac{1}{3}d^2} \right] dR \\ \mu dD_G t + F(R_0) &= D_C R + \frac{d(2D_G - D_C)}{2} \ln(R^2 - dR + \frac{1}{3}d^2) + \frac{5}{3}dD_C\sqrt{3} \arctan\left(2\sqrt{3}\left(\frac{R}{d} - \frac{1}{2}\right)\right) \end{aligned}$$

Therefore,

$$\mu dD_G t + F(R_0) = D_C R + \frac{d(2D_G - D_C)}{2} \ln(R^2 - dR + \frac{1}{3}d^2) + \frac{5}{3}dD_C\sqrt{3} \arctan\left(2\sqrt{3}\left(\frac{R}{d} - \frac{1}{2}\right)\right) \quad (2.2.3)$$

where F is defined by the right-hand side of 2.2.3.

From 2.2.3 will see that $R(t)$ is defined for $t > 0$. Indeed, $\frac{5}{3}dD_C\sqrt{3} \arctan\left(2\sqrt{3}\left(\frac{R}{d} - \frac{1}{2}\right)\right)$ is bounded. In addition,

$$\lim_{R \rightarrow \infty} \left[D_C R + \frac{d(2D_G - D_C)}{2} \ln(R^2 - dR + \frac{1}{3}d^2) \right] = \lim_{R \rightarrow \infty} R \left[D_C + \frac{d(2D_G - D_C)}{2} \frac{\ln(R^2 - dR + \frac{1}{3}d^2)}{R} \right],$$

and, using L'Hopital's rule[54], we have

$$\begin{aligned} \lim_{R \rightarrow \infty} \frac{\ln(R^2 - dR + \frac{1}{3}d^2)}{R} &= \lim_{R \rightarrow \infty} \frac{2R - d}{R^2 - dR + \frac{1}{3}d^2} \\ &= 0. \end{aligned}$$

Hence,

$$\lim_{R \rightarrow \infty} \left[D_C + \frac{d(2D_G - D_C)}{2} \frac{\ln(R^2 - dR + \frac{1}{3}d^2)}{R} \right] = D_C$$

Therefore, by product of limits, we have:

$$\lim_{R \rightarrow \infty} R \left[D_C + \frac{d(2D_G - D_C)}{2} \frac{\ln(R^2 - dR + \frac{1}{3}d^2)}{R} \right] = \infty$$

Thus, we have,

$$\lim_{R \rightarrow \infty} \left[D_C R + \frac{d(2D_G - D_C)}{2} \ln \left(R^2 - dR + \frac{1}{3}d^2 \right) + \frac{5}{3}dD_C\sqrt{3} \arctan \left(2\sqrt{3} \left(\frac{R}{d} - \frac{1}{2} \right) \right) \right] = \infty$$

From the previous and 2.2.3, we see that $R(t)$ is finite for t finite. Hence, the solution of 2.1.11 is defined for $t \geq 0$ [56].

In addition, since $g(r) > 0$, and $f(r) > 0$ for $r \in \mathbb{R}$,

$$\frac{dR}{dt} > 0; \quad t \geq 0 \tag{2.2.4}$$

So, $R(t)$ is strictly monotone increasing for $t \geq 0$, and 2.1.11 has no steady states.

It follows that $\lim_{t \rightarrow \infty} R(t) = \infty$.

2.3 Instantaneous Doubling Time for Small and Large Tumors

For comparison to empirical data, it is interesting to consider the doubling time for tumor volume in large and small tumors. For this, consider 2.1.13.

In small tumor where $R < d$ we have

$$\left[\frac{d}{dR}(R'(t)) \right]_{R=d} = \frac{1}{3}\mu$$

Thus, for small R , $R'(t)$ is :

$$R'(t) = \frac{1}{3}\mu R \quad (2.3.1)$$

We then define the doubling time of the radius of the nascent tumor, t_R , by:

$$t_R = \frac{3 \ln 2}{\mu} \quad (2.3.2)$$

Now we find the doubling time of the volume, t_V , of the nascent tumor:

$$\begin{aligned} V &= \frac{4}{3}\pi R^3 \\ V'(t) &= 4\pi R^2 R'(t) \\ V'(t)|_{R=d} &\approx \frac{4}{3}\pi d^3 \mu \\ &= \mu V \end{aligned}$$

Thus the doubling time of the volume, t_V , of the nascent tumor is:

$$t_V = \frac{\ln 2}{\mu} \quad (2.3.3)$$

Some studies define the doubling time of the tumor as $\frac{\ln 2}{SGR}$, where SGR stands for the Specific Growth Rate [37]. This is similar to our model for a small tumor.

Now we consider the growth of the tumor volume when R is very large.

Define R'_∞ by:

$$\begin{aligned} R'_\infty &:= \lim_{R \rightarrow \infty} R'(t) \\ &= \frac{\mu d D_G}{D_C} \end{aligned}$$

Thus when R is very large, the growth rate of the tumor volume is approximated as follows:

$$\begin{aligned} V' &= 4\pi R^2 R' \\ &= 4\pi R^2 \frac{\mu d D_G}{D_C} \\ &= V \frac{3\mu d D_G}{R D_C} \\ &= (36\pi)^{\frac{1}{3}} \mu d \frac{D_G}{D_C} V^{\frac{2}{3}} \end{aligned}$$

From the final expression, we see that the growth of a large tumor is less than exponential. In addition, from the second-to-last expression, we see that in a large tumor the growth rate per unit volume scales with $\frac{d}{R}$, so we may define the instantaneous doubling time of a large tumor as:

$$t^* = \frac{\ln 2}{3\mu} \left(\frac{D_C}{D_G} \right) \left(\frac{R}{d} \right) \quad (2.3.4)$$

Hence, when the tumor is large, the instantaneous doubling time increases with tumor radius.

For small tumors we observe that the model tumor radius and volume increases exponentially, but for large tumors, the model tumor radius increases linearly and the volume increases approximately sub exponentially. Pérez-García et al observed different types of tumors can exhibit different types of volume growth in vivo; e.g., super-exponential, exponential, and linear, etc [49]. In general, the potential tumor doubling time is shorter than the observed doubling time in vivo [37], which is consistent with a model in which the rate of growth slows through time.

CHAPTER 3

NATURAL KILLER CELLS IN BREAST CANCER, BACKGROUND

Natural Killer cells (NK cells) are lymphocytes, that is, immune cells that originate in the bone marrow, circulate through the blood, and patrol peripheral tissues [50, 28, 4]. NK cells are distinguished among lymphocytes in their ability to detect and eliminate cancer cells without prior sensitization [26, 28]. Indeed, they are considered part of the innate immune system [50, 9, 33, 59, 23, 1, 57]. NK cells can also help orchestrate tissue remodeling and angiogenesis [8, 50]. Indeed, a multitude of NK cell phenotypes supports a wide range of functions in diverse tissues and contexts. It has been proposed that cancer tissues subvert the immune system, in part, by exploiting the NK cells ability to promote healing, and the interplay between NK cells and cancer cells is thought to be critical for determining the propensity of the cancer to grow and invade [9].

In the following subsection we describe research on the function and activity of NK cells in breast cancer, with special focus on HER2+ breast cancer and explain how the available knowledge is translated into a simplified model.

3.1 NK cell range/specificity

Even within a single tumor, cancer cells differ in their susceptibility to NK cell killing. In the context of HER2+ breast cancer, studies suggest that NK cells are severely limited in their ability to inhibit tumor growth. The addition of a therapeutic antibody, trastuzumab, exposes the tumor to NK cell attack. However, even in the presence of trastuzumab, NK cell cytotoxicity is limited to the tumor periphery [55]. We interpret the inability of NK cells to penetrate the tumor matrix as a manifestation of differences between cells in the tumor interior and cells in the tumor periphery. Indeed, using mouse models of breast cancer, Cheung et al. [11, 10] identified a marker of invasive and proliferative potential in the breast cancer cells (Katerin-14 (K-14)), which is "enriched at the tumor's invasive borders," [10] and characterizes the subpopulation of cells that are susceptible to NK cell attack [9]. As a result of these considerations, our model supposes that NK cells only destroy tumor cells in the peripheral growth region of the tumor. See Figure 2B in [55] for a schematic of NK cell specificity and activity with and without therapeutic antigen.

3.2 NK cell type, activation, and exhaustion/subversion by the tumor

NK cells vary in their ability to destroy cancer cells. In our model, we distinguish two type of NK cells: cytotoxic NK cells which are capable of killing cancer cells, and noncytotoxic NK cells, which are unable to kill cancer cells [1]. It is suggested that noncytotoxic NK cells can differentiate into cytotoxic NK cells through exposure to activating signals [8]. However, we do not include the complex process of NK cell differentiation in our model as it is unclear if differentiation from noncytotoxic to cytotoxic NK cell subset can occur in tissues [8, 50]. The cytotoxic potential of NK cells can be enhanced through exposure to cytokines produced by adaptive immune cells, such as IL-2 or IL-15 [9, 59], or through exposure to cancer cells [50, 28]. Our model does not include the adaptive immune response, so we assume trastuzumab-treated tumor cells directly enhance cytotoxicity in the cytotoxic NK cell subgroup. Thus, we include two classes of cytotoxic NK cells: resting cytotoxic NK cells ($[NK]_c$) and tumor-activated cytotoxic NK cells ($[NK]^*$). The biological literature suggests NK cells typically die post activation. However, in some contexts, a minority of active NK cells may be maintained in a state of heightened sensitivity to protect against similar threats in the future [46].

Although initial exposure to cancer cells can induce cytotoxicity, long term exposure can leave NK cells in a noncytotoxic, exhausted state [33, 9, 10]. In one study, overnight exposure to tumor cells significantly impaired the cytotoxic potential of NK cells and promoted apoptosis [33]. In the context of breast cancer, Chan et al. found that after 3 to 4 days of exposure to cancer cells, NK cells lost their cytotoxicity [9]. The process by which tumor cells disarm NK cells is complex, studies suggest that after prolonged contact with tumor cells, NK cells first lose their toxicity [9, 5, 11], and then become inactive or exhausted [9]. Exhausted NK cells may remain around the tumor site and can even be reprogrammed to promote tumor invasion cells [9, 50], although we do not describe the cancer-promoting potential of exhausted NK cells in our model. To account for NK exhaustion, we include two classes of noncytotoxic NK cells in our model: noncytotoxic NK cells ($[NK]_n$) and exhausted NK cells ($[NK]_e$).

3.3 NK cell recruitment

NK cells can be found in most tissues, although the number and activation profile of the cells varies with the tissue type [50, 8]. Disease, including cancer, can lead to NK cell recruitment [28] and alter the distribution of NK cell types within a tissue [50, 8]. In some contexts, cancer can activate NK cell cytotoxicity. Specifically, tumor cells can stimulate NK cells to produce chemokines and cytokines that attract additional immune cells, NK cells included, to the tumor site [28], and co-culture with cancer cells can induce NK cell proliferation [46, 25]. The expansion of the NK cell population in response to disease is typically short lived due to the limited proliferative potential of these cells [25]. Indeed, NK cell proliferation in response to antigen presentation is proposed to be limited by concomitant telomere shortening [52]. Our model assumes that NK cell infiltration of the tumor site is supported by initial activation and subsequent immigration of NK cells from the blood, and/or proliferation of resident cytotoxic NK cells. In addition, cancer has been shown to alter the expression of chemokines within breast tissue, thereby increasing the proportion of NK cells that are noncytotoxic [8, 50]. For this reason, we also include NK cell recruitment by cancerous and healthy tissue in our model.

CHAPTER 4

A MODEL OF NK CELLS WITHIN A TUMOR

In this section we describe our mathematical model of tumor growth in the presence of trastuzumab.

4.1 Modeling NK Cells Killing and Activation

We model NK cell killing of tumor cells as a two-part process that consists of the NK cell contacting and subsequently killing a tumor cell. The rate of contact with tumor cells depends on the velocity of the NK cells and the density of tumor cells in the region, and the rate of killing, given contact, is taken as the maximal kill rate observed in the literature. Studies show that NK cell velocity depends on the presence of stimulating ligands, so that NK cells move more quickly in the presence of such ligands [18]. Based on this research we take the velocity of active NK cells, v_{NK}^* , as $5.2 \cdot 10^{-3} \text{ mm min}^{-1}$, and the velocity of nonactive NK cells, v_{NK} , as $1.6 \cdot 10^{-3} \text{ mm min}^{-1}$ [18]. Additionally, since active NK cells are observed to kill in as little as ten minutes [18], while inactive NK cells require at least 4 hours to kill [1], we let the max kill rate for inactive cells, δ , be 0.0042 min^{-1} and the max kill rate for active cells, δ^* , be 0.1 min^{-1} . The observed kill rate is then determined from the density of NK cells, the maximal kill rate, and the velocity of NK cells as follows. Letting $[NK]_c$ be the density of non-active, cytotoxic NK cells and $[NK]^*$ be the density of active cytotoxic NK cells, the volume occupied by a single non-active NK cell per unit time (V), and the volume occupied by a single active NK cell per unit time (V^*) are estimated as

$$V = \pi r_{NK}^2 v_{NK}, \quad (4.1.1)$$

and

$$V^* = \pi r_{NK}^2 v_{NK}^*, \quad (4.1.2)$$

where r_{NK} is the radius of an NK cell, the shape of an NK cell is approximated as a sphere, and the occupied area is approximated as a cylinder. Then, $V D_G$ represents the number of tumor cells a cytotoxic NK cell contacts per unit time, and $V^* D_G$

represents the number of tumor cells an active cytotoxic NK cell contacts per unit time. Therefore, the NK cell killing rate (kills per day) of active NK cells, ξ^* , is given as:

$$\xi^* = [NK]^* \frac{\delta^* V^* D_G}{\delta^* + V^* D_G} \times V_G = [NK]^* \frac{\delta^* V^* T_G}{\delta^* + V^* D_G}, \quad (4.1.3)$$

where V_G is the volume of the growth region in which we assume the NK cells are located (see 2.1.5). Similarly, the killing rate (kills per day) of non-active NK cells, ξ , is defined as:

$$\xi = [NK]_c \frac{\delta V D_G}{\delta + V D_G} \times V_G = [NK]_c \frac{\delta V T_G}{\delta + V D_G} \quad (4.1.4)$$

Finally, as described previously (see section 3.2), our model assumes trastuzumab-treated tumor cells directly activate cytotoxicity in the the cytotoxic NK cell subgroup. Specifically, we suppose that inactive NK cells become active through the process of tumor cell contact and killing, and take the rate of cytotoxic NK cell activation as $\frac{\xi}{V_G}$.

4.2 Recruitment of NK cells

As described in section 3.1, cancerous and healthy tissues recruit NK cell to the tumor region, with cancerous tissue promoting an increase in the proportion of NK cells that are cytotoxic [8, 50]. While some researchers propose that cancer does not necessarily impact the density of NK cells within a tissue [8], other research supports increased recruitment of NK cells to cancerous tissue [28]. We reconcile these observations within our model by supposing that in the absence of NK cell activation, cancerous tissue alters the distribution of NK cells types without altering the total density of NK cells. We propose the following, model of NK cell recruitment. Let b_n be the recruitment rate of noncytotoxic NK cells and b_c be the recruitment rate of cytotoxic NK cells. We set

$$b_n = \frac{\alpha_2 K_1 + \alpha_3 D_G}{K_1 + D_G},$$

and

$$b_c = \frac{\alpha_1 K_1}{K_1 + D_G},$$

where the constraint

$$\alpha_3 = \alpha_1 + \alpha_2, \tag{4.2.1}$$

ensures the total density of NK cells is preserved. Assuming NK cells leave the tumor region at a constant per capita rate β , which is determined by the life expectancy of an NK cell, we arrive at the following differential equations for describing NK cell recruitment and removal in the absence of activation by the tumor:

$$\frac{d}{dt}[NK]^c = \frac{\alpha_1 K_1}{K_1 + D_G} - \beta[NK]^c \tag{4.2.2}$$

$$\frac{d}{dt}[NK]^n = \frac{\alpha_2 K_1 + \alpha_3 D_G}{K_1 + D_G} - \beta[NK]^n. \tag{4.2.3}$$

From (4.2.2) and (4.2.3) we find the steady-state concentrations of cytotoxic NK cells

$$\overline{[NK]}^c = \frac{\alpha_1}{\beta} \frac{K_1}{K_1 + D_G}, \tag{4.2.4}$$

noncytotoxic NK cells

$$\overline{[NK]_n} = \frac{\alpha_2 K_1 + \alpha_3 D_G}{\beta (K_1 + D_G)}, \quad (4.2.5)$$

and total NK cells

$$\overline{[NK]_T} = \frac{\alpha_3}{\beta}. \quad (4.2.6)$$

The parameter α_3 is then determined from the life expectancy of an NK cell (14 days [38]) and the density of NK cells in healthy tissue. NK cell density in healthy tissue is estimated from [50] and [18] as 500 cells mm^{-3} . Specifically, Ran et al report NK cell density in healthy tissue as 100 cells mm^{-2} [50], and Deguine et al report NK cell density in antigen free-tumor as 300 cells/ mm^2 [18].

$$\alpha_3 = 500 \beta$$

The parameters α_1 , α_2 , and K_1 are determined from (4.2.1), (4.2.4 - 4.2.5), and the steady-state ratios of cytotoxic to noncytotoxic NK cells in healthy and cancerous breast tissue: In healthy breast tissue (where $D_G = 0$) we set $\frac{[NK]^c}{[NK]_n} = \frac{0.96}{0.04}$, while in cancerous breast tissue (where $D_G = 10^5$ Cell mm^{-3} [19]) we set $\frac{[NK]^c}{[NK]_n} = \frac{0.7}{0.3}$ [8]. These constraints give

$$\frac{\alpha_1}{\alpha_2} = \frac{0.96}{0.04},$$

so that

$$\alpha_1 = 0.96 \alpha_3,$$

$$\alpha_2 = 0.04 \alpha_3,$$

and K_1 is determined from

$$\frac{\alpha_1 K_1}{\alpha_2 K_1 + \alpha_3 D_G} = \frac{0.7}{0.3}.$$

4.3 Modeling NK population expansion through immune system activation

Now we describe a model for recruitment of cytotoxic NK cells through tumor-induced NK cell activation and subsequent proliferation and immigration (see section 3.3). Since NK cells are the only immune cells included in our simplified model, we suppose that tumor-activated cytotoxic NK cells directly recruit active cytotoxic NK cells, although, in reality additional immune cell types can contribute to this process. Specifically, we suppose active cytotoxic NK cells recruit active cytotoxic NK cells with a constant per capita rate r . This recruitment is potentially the result of immigration to the tumor site from the blood and/or proliferation of activated NK cells. Research suggests that under activating conditions the density of NK cells in a tissue can increase 5-10 fold within a few days [28]. In addition, Fujisaki et al. found that seven-day coculture with "engineered" cancer cells produced an average 21.6-fold expansion of NK cells from peripheral blood (5.1- 86.6-fold; $n = 50$) [25]. As a baseline, we suppose a 5 fold increase in 2 days, and define the per capita recruitment rate as;

$$r = \frac{\ln 5}{2 \cdot 24 \cdot 60} . \quad (4.3.1)$$

Since, NK cells are limited in their potential to proliferate post activation, we include a separate compartment for newly created NK cells ($[NK]_p^*$). We suppose these cells are short lived and unable to proliferate [25]. The death rate of these NK cells is denoted as β_p .

4.4 Tumor-induced exhaustion of active cytotoxic NK cells

In this section we describe our model of tumor-induced NK cell exhaustion. Although the exhausted NK cells may have shorter lifespans and tumor-promoting potential (see section 3.2) we do not incorporate these features into our model. We treat exhausted NK cells as a noncytotoxic NK cell subset that cannot be revitalized. As such, exhaustion serves a sink for NK cells. We suppose that under continuous exposure to cancer cells, NK cells become exhausted at a maximal per capita rate γ . As a baseline, we set the maximal time to exhaustion as one day (see section 3.2). Then, a parameter K_2 controls the sensitivity of the exhaustion response to tumor cells, so that the per capita rate of exhaustion at tumor density D is

$$E^* = \gamma \frac{D}{K_2 + D}.$$

Here K_2 determines the sensitivity of the exhaustion response to tumor cells. We are unable to estimate K_2 from the biological literature, so we express K_2 as a proportion of the maximal tumor density and vary the proportion during numerical simulations.

4.5 Differential equations for NK cells in the presence of immune system activation

$$\frac{d}{dt}[NK]^c = \frac{\alpha_1 K_1}{K_1 + D_G} - [NK]^c \frac{\delta V D_G}{\delta + V D_G} - \beta [NK]^c \quad (4.5.1)$$

$$\frac{d}{dt}[NK]^* = [NK]^c \frac{\delta V D_G}{\delta + V D_G} - \left(\beta + \gamma \frac{D_G}{K_2 + D_G} \right) [NK]^* \quad (4.5.2)$$

$$\frac{d}{dt}[NK]_p^* = r [NK]^* - \beta_p [NK]_p^* \quad (4.5.3)$$

$$\frac{d}{dt}[NK]_e = \gamma \frac{D_G}{K_2 + D_G} [NK]^* - \beta [NK]_e \quad (4.5.4)$$

From 4.5.1 - 4.5.4, we find the steady-states of different concentrations of cytotoxicity NK cells in the presence of immune system activation

$$\overline{[NK]^c} = \frac{b_c (\delta + V D_G)}{\beta \delta + V D_G (\delta + \beta)}, \quad (4.5.5)$$

$$\overline{[NK]^*} = \frac{b_c \delta V D_G}{(\beta + E^*) (\beta \delta + V D_G (\delta + \beta))}, \quad (4.5.6)$$

$$\overline{[NK]_p^*} = \frac{r}{\beta_p} \overline{[NK]^*}, \quad (4.5.7)$$

and

$$\overline{[NK]_e} = \frac{E^*}{\beta} \overline{[NK]^*} \quad (4.5.8)$$

(4.5.5 - 4.5.8) will be useful in subsequent qualitative analysis.

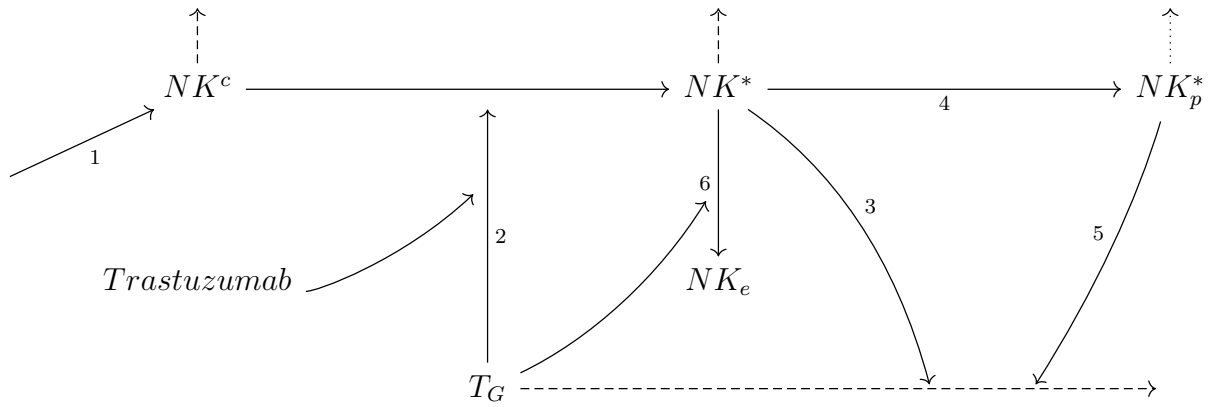


Figure 2: Schematic for NK cell dynamics in the presence of tumor-induced immune system activation. 1. Cytotoxic NK cells are recruited to the tissue from the blood. 2. In the presence of trastuzumab, tumor cells activate NK cells. 3. Tumor-activated NK cells kill tumor cells and 4. recruit additional active, cytotoxic NK cells to the tumor site. 5. Newly recruited NK cells contribute to tumor cell killing. 6. In the presence of tumor cells, tumor-activated cytotoxic NK cells gradually become exhausted. Legend: NK^c : cytotoxic NK cells, NK^* : active, NK_p^* : newly recruited, cytotoxic NK cells, NK_e : exhausted NK cells, T_G : tumor cells in the growth region.

CHAPTER 5

**A MODEL OF TUMOR GROWTH WITH DRUG-INDUCED
IMMUNE SYSTEM ACTIVATION**

In this section we incorporate immune system activation into our tumor growth model. Our model of immune system activation is specific for trastuzumab treatment of HER2+ breast cancer, wherein trastuzumab functions to expose cancer cells on the tumor's periphery to NK cell killing. The effect of trastuzumab treatment is to alter our conservation law, since now tumor cells in the growth region are removed through killing by cytotoxic NK cells. In this model, the rate of tumor cell population growth is:

$$\mu T_G - \xi - \xi^* = \begin{cases} \frac{d(T_C + T_G)}{dt}, & R \geq d \\ \frac{dT_G}{dt}, & R < d \end{cases} \quad (5.0.9)$$

Let's suppose $R \geq d$, that is,

$$\frac{d(T_C + T_G)}{dt} = \mu T_G - [NK]^c \frac{\delta V}{\delta + V D_G} T_G - [NK]^*_T \frac{\delta^* V^*}{\delta^* + V^* D_G} T_G. \quad (5.0.10)$$

This yields the conservation equation.

$$4\pi [D_C R^2 - 2d(D_C - D_G)R + d^2(D_C - D_G)] \frac{dR}{dt} = \mu T_G - [NK]^c \frac{\delta V}{\delta + V D_G} T_G - [NK]^*_T \frac{\delta^* V^*}{\delta^* + V^* D_G} T_G \quad (5.0.11)$$

Defining φ , ϕ , and ψ by:

$$\varphi = \mu V V^*, \quad (5.0.12)$$

$$\phi = \mu(\delta^* V + \delta V^*) - \delta V V^* [NK]^c - \delta^* V V^* [NK]^*_T, \quad (5.0.13)$$

and

$$\psi = \mu \delta \delta^* - \delta \delta^* V [NK]^c - \delta \delta^* V^* [NK]^*_T, \quad (5.0.14)$$

we can observe that

$$\mu T_G - [NK]_c \frac{\delta V}{\delta + VD_G} T_G - [NK]_T^* \frac{\delta^* V^*}{\delta^* + V^* D_G} T_G = \frac{\varphi D_G^2 + \phi D_G + \psi}{(\delta + VD_G)(\delta^* + V^* D_G)} T_G \quad (5.0.15)$$

so 5.0.11 becomes

$$4\pi [D_C R^2 - 2d(D_C - D_G)R + d^2(D_C - D_G)] \frac{dR}{dt} = 4\pi d D_G \frac{\varphi D_G^2 + \phi D_G + \psi}{(\delta + VD_G)(\delta^* + V^* D_G)} \left[R^2 - Rd + \frac{1}{3}d^2 \right]. \quad (5.0.16)$$

We let H be defined as follows:

$$H = d D_G \frac{\varphi D_G^2 + \phi D_G + \psi}{(\delta + VD_G)(\delta^* + V^* D_G)}. \quad (5.0.17)$$

Thus,

$$\frac{dR}{dt} = H \frac{R^2 - Rd + \frac{1}{3}d^2}{D_C R^2 - 2d(D_C - D_G)R + d^2(D_C - D_G)}, \quad R \geq d. \quad (5.0.18)$$

We do the same for $R < d$ and we have

$$\frac{dR}{dt} = \begin{cases} H \frac{R^2 - Rd + \frac{1}{3}d^2}{D_C R^2 - 2d(D_C - D_G)R + d^2(D_C - D_G)}, & R \geq d \\ \frac{1}{3}HR, & R < d \end{cases}. \quad (5.0.19)$$

From the previous, we have the following system of differential equations to model tumor growth with immune system activation:

$$\left\{ \begin{array}{l} \frac{d}{dt}[NK]^c = \frac{\alpha_1 K_1}{K_1 + D_G} - [NK]^c \frac{\delta V D_G}{\delta + V D_G} - \beta [NK]^c \\ \frac{d}{dt}[NK]_n = \frac{\alpha_2 K + \alpha_3 T_G}{K + T_G} - \beta [NK]_n \\ \frac{d}{dt}[NK]_e = \gamma \frac{D_G}{K_2 + D_G} [NK]^* - \beta [NK]_e \\ \frac{d}{dt}[NK]_p^* = r [NK]^* - \beta_p [NK]_p^* \\ \frac{d}{dt}[NK]^* = [NK]^c \frac{\delta V D_G}{\delta + V D_G} - \left(\beta + \gamma \frac{D_G}{K_2 + D_G} \right) [NK]^* , \end{array} \right. \quad (5.0.20)$$

and

$$\left\{ \begin{array}{l} \frac{d}{dt} T_G = \begin{cases} 4\pi d D_G (2R - d) \frac{dR}{dt}, & R \geq d \\ 4\pi D_G R^2 \frac{dR}{dt}, & R < d \end{cases} \\ \frac{d}{dt} T_C = \begin{cases} 4\pi D_C (R(t) - d)^2 \frac{dR}{dt}, & R \geq d \\ 0, & R < d \end{cases} \\ \frac{dR}{dt} = \begin{cases} H \frac{R^2 - Rd + \frac{1}{3}d^2}{D_C R^2 - 2d(D_C - D_G)R + d^2(D_C - D_G)}, & R \geq d \\ \frac{1}{3}HR, & R < d \end{cases} \end{array} \right. , \quad (5.0.21)$$

with H defined in 5.0.17.

CHAPTER 6

**QUALITATIVE ANALYSIS OF THE MODEL OF TUMOR GROWTH
WITH IMMUNE SYSTEM ACTIVATION**

In this section, we give a qualitative analysis of the tumor growth model with trastuzumab-induced immune system activation. First let's consider the potential for model steady-states.

Consider how the sign of $\frac{dR}{dt}$ varies with the parameter α_1 . Note that when $\alpha_1 = 0$, $\overline{[NK]}^c = 0$ and $\overline{[NK]}_T^* = 0$. Hence, in this case, the tumor grows as in the absence of immune system activation. In particular, $\frac{dR}{dt} > 0$ as in section 2.2 and $\lim_{t \rightarrow \infty} R(t) = \infty$. On the other hand, as α_1 approaches infinity, both ϕ and ψ approach negative infinity, so H approaches negative infinity as well. Hence, for α_1 large, $\frac{dR}{dt} < 0$, and, by the intermediate value theorem, there exists a critical value of α_1 for which $\frac{dR}{dt} = 0$. Moreover, since α_1 determines the steady-state level of cytotoxic NK cells in that absence of activation, this result implies that if healthy tissue has high levels of patrolling NK cells, then the tumor can not exist.

Next we consider how the sign of $\frac{dR}{dt}$ varies with the parameter V . If $V = 0$, then $\overline{[NK]}_T^* = 0$, and no tumor cell killing occurs. Hence, the tumor grows as in the absence of immune system activation, $\frac{dR}{dt} > 0$, and $\lim_{t \rightarrow \infty} R(t) = \infty$ as in section 2.2. On the other hand, in the limit as V approaches infinity, $\overline{[NK]}^c = \frac{b_c}{(\delta + \beta)}$, and $\overline{[NK]}_T^* = \frac{b_c \delta}{(\delta + \beta)(\beta + E^*)} \left(1 + \frac{r}{\beta_p}\right)$. Substituting these expressions into the left-hand-side of (5.0.15), we find that

$$H = \frac{d}{\delta^* + V^* D_G} \left[\mu(V^* D_G^2 + \delta^* D_G) - \frac{\delta b_c V^* D_G}{\beta + \delta} - \frac{\delta \delta^* V^* b_c D_G}{(\delta + \beta)(\beta + E^*)} \left(1 + \frac{r}{\beta_p}\right) - \frac{b_c \delta \delta^*}{\delta + \beta} \right].$$

We conclude that $H < 0$, and hence $\frac{dR}{dt} < 0$, if and only if

$$\mu < \left[\frac{\delta b_c V^* D_G}{\beta + \delta} + \frac{\delta \delta^* V^* b_c D_G}{(\delta + \beta)(\beta + E^*)} \left(1 + \frac{r}{\beta_p}\right) + \frac{b_c \delta \delta^*}{\delta + \beta} \right] \frac{1}{V^* D_G^2 + \delta^* D_G}.$$

The sign of H varies similarly with D_G . (Notice that the expression inside the parenthesis of H is quadratic in D_G with positive discriminant.) Thus, we cannot control aggressive tumors (those with very fast proliferation or high density) by

increasing the velocity of NK cells.

Next we consider how the sign of $\frac{dR}{dt}$ varies with the parameter δ . If $\delta = 0$, then $H = \mu dD_G$, and no tumor cell killing occurs. Hence, the tumor grows as in the absence of immune system activation, $\frac{dR}{dt} > 0$, and $\lim_{t \rightarrow \infty} R(t) = \infty$ as in section 2.2. As δ goes to infinity, $[\overline{NK}]_c = \frac{b_c}{\beta + VD_G}$, and $[\overline{NK}]_T^* = \frac{VD_G b_c}{(\beta + e^*)(\beta + VD_G)} (1 + \frac{r}{\beta_p})$. Substituting these expression into the left-hand-side of (5.0.15), we find that

$$H = \frac{dD_G}{\delta^* + V^*D_G} \left[\mu(V^*D_G + \delta^*) - \frac{b_c VV^*D_G}{\beta + VD_G} - \frac{\delta^* VV^*D_G b_c}{(\beta + E^*)(\beta + VD_G)} (1 + \frac{r}{\beta_p}) - \frac{b_c \delta^* V}{\beta + VD_G} \right]$$

Hence, $H < 0$, and $\frac{dR}{dt} < 0$, if and only if

$$\mu < \left[\frac{b_c VV^*D_G}{\beta + VD_G} + \frac{\delta^* VV^*D_G b_c}{(\beta + E^*)(\beta + VD_G)} (1 + \frac{r}{\beta_p}) + \frac{b_c \delta^* V}{\beta + VD_G} \right] \frac{1}{V^*D_G + \delta^*} .$$

Thus the analysis for δ is similar to V ; we cannot control aggressive tumors by increasing the killing rate of NK cells. In summary, the analyses of δ and V show that increasing the cytotoxicity of patrolling NK cells may be insufficient for the control of highly aggressive tumors.

Finally we consider how the sign of $\frac{dR}{dt}$ varies with the parameter r . Notice that as r approaches infinity, $[\overline{NK}]_T^*$ approaches infinity, and hence H approaches negative infinity. Hence, for r large, $\frac{dR}{dt} < 0$. That is for r large, the tumor is shrinking. On the other hand, if $r = 0$, we have

$$H = \frac{dD_G}{(\delta + VD_G)(\delta^* + V^*D_G)} \left[\mu(VV^*D_G^2 + (\delta^*V + \delta V^*)D_G + \delta\delta^*) - \frac{b_c(\delta VV^* + \delta\delta^*V)(\delta + VD_G)}{\beta\delta + VD_G(\delta + \beta)} - \frac{b_c\delta VD_G(\delta^*VV^* + \delta\delta^*V)}{(\beta + E^*)(\beta\delta + VD_G(\delta + \beta))} \right]$$

We conclude that $H < 0$, and hence $\frac{dR}{dt} < 0$, if and only if

$$\mu < \left[\frac{b_c(\delta VV^* + \delta\delta^*V)(\delta + VD_G)}{\beta\delta + VD_G(\delta + \beta)} + \frac{b_c\delta VD_G(\delta^*VV^* + \delta\delta^*V)}{(\beta + E^*)(\beta\delta + VD_G(\delta + \beta))} \right] \frac{1}{VV^*D_G^2 + (\delta^*V + \delta V^*)D_G + \delta\delta^*} .$$

In summary, depending on the values of the remaining parameters, the tumor may grow or shrink in the absence of NK cell proliferation, and even highly aggressive tumors can be eliminated by driving the rate of NK cell proliferation large.

CHAPTER 7

NUMERICAL SIMULATIONS

In this section, we test our model's ability to describe tumor volume data from patients with untreated hamartomas [49]. It should be noted that hamartomas are not technically tumors, but atypical masses of predominantly normal cells [41]. However, because hamartomas are typically benign, it is possible to obtain data on untreated hamartomas over long periods of time. Hence, for reasons of data availability, we initially test our model on hamartoma data. We fit two model parameters: the per capita growth rate, μ , and the diameter of the growth region, d , to the data by minimizing the squared error between the data and the model output.

Looking at figures 3-8, we see that our model provides an accurate description of many patient data sets. In addition, we see that model fits suggest the rate of volume increase in patient hamartomas spanned the exponential and sub exponential regimes of our model.

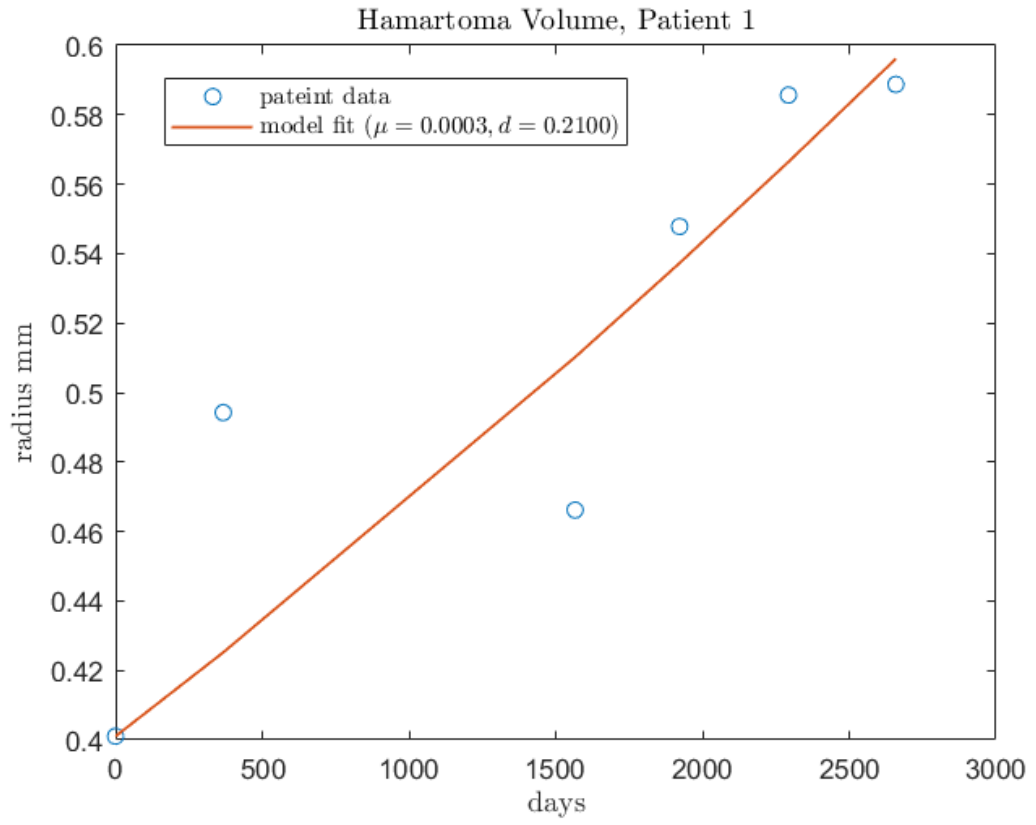


Figure 3: Hamartoma Volume Patient 1.

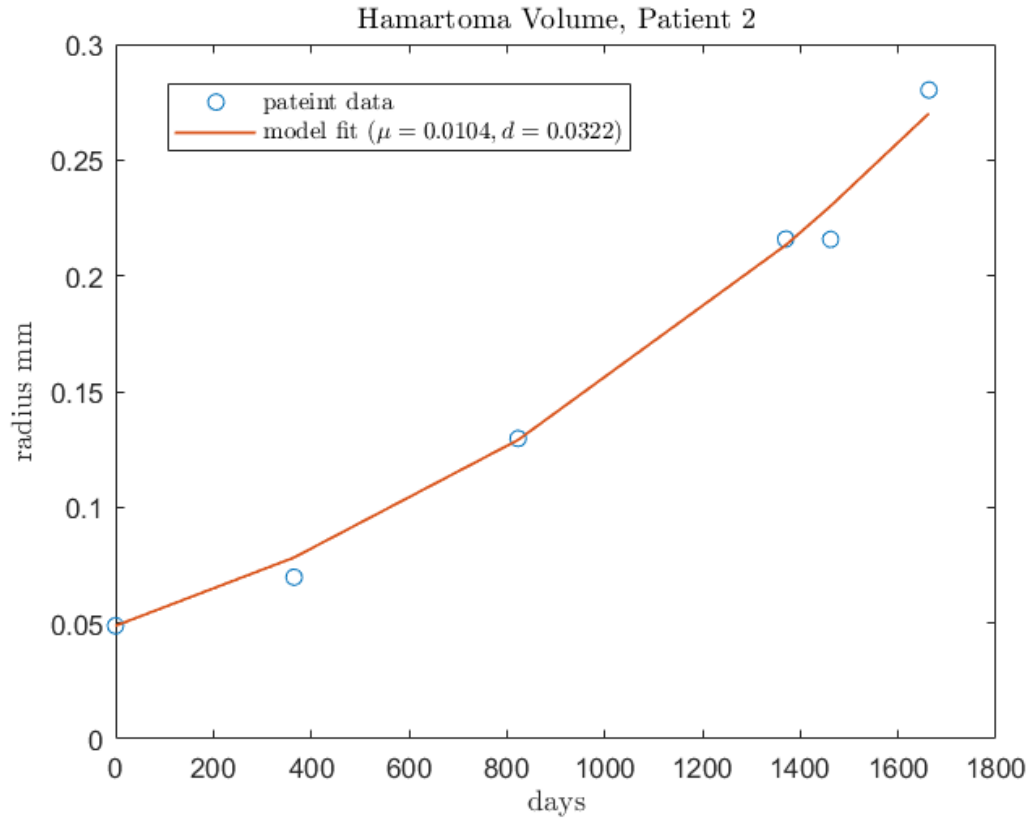


Figure 4: Hamartoma Volume Patient 2.

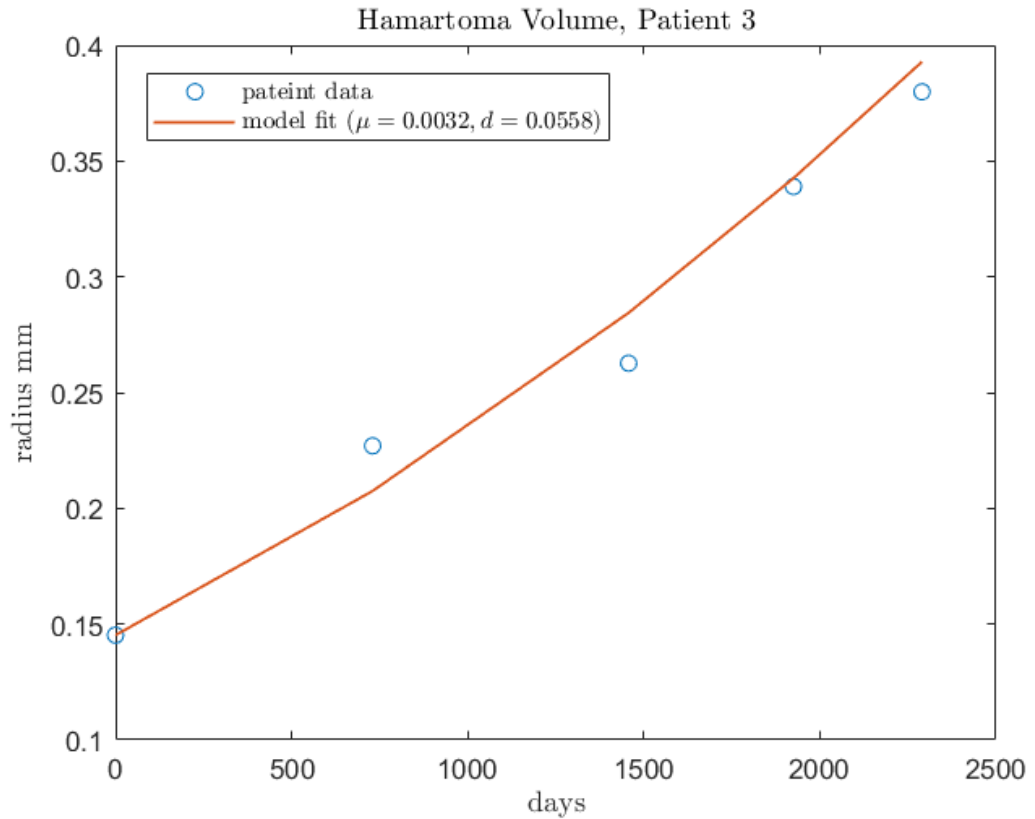


Figure 5: Hamartoma Volume Patient 3.

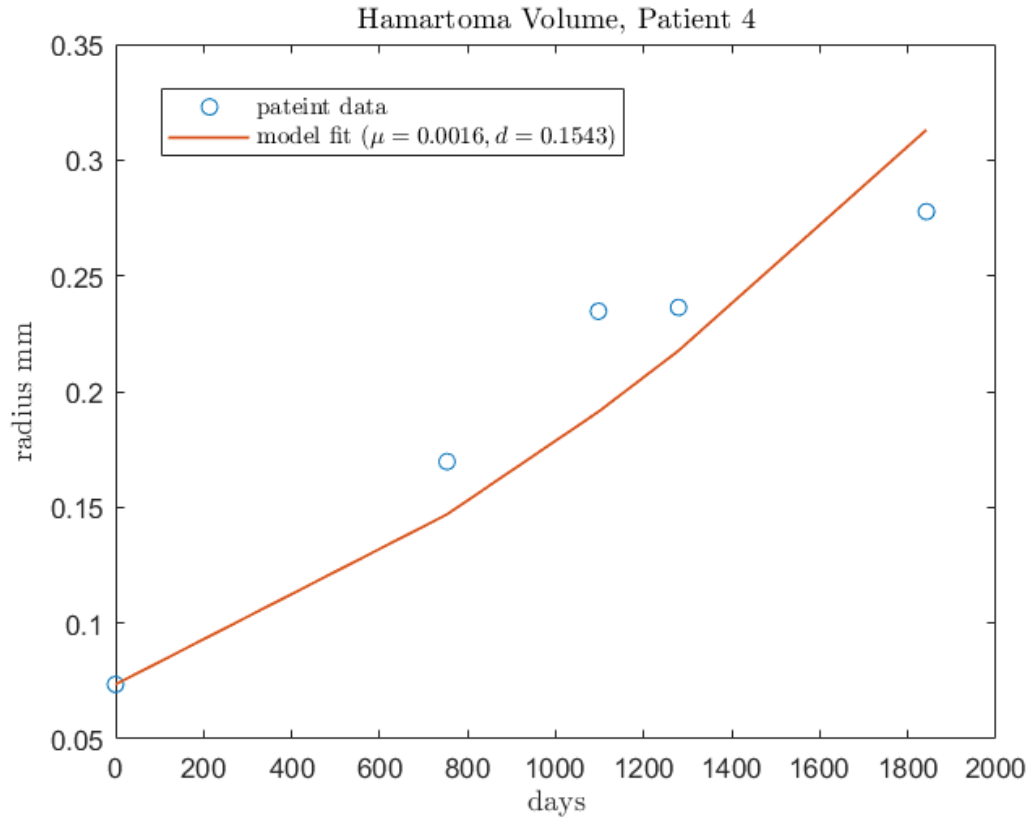


Figure 6: Hamartoma Volume Patient 4.

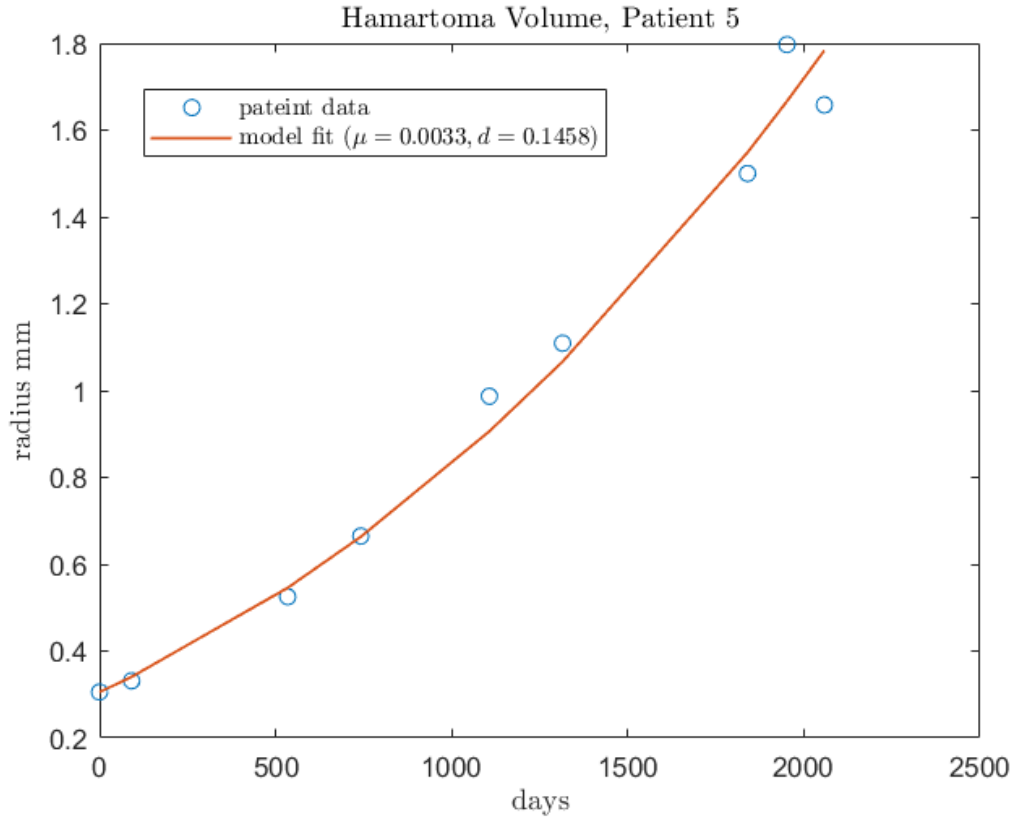


Figure 7: Hamartoma Volume Patient 5.

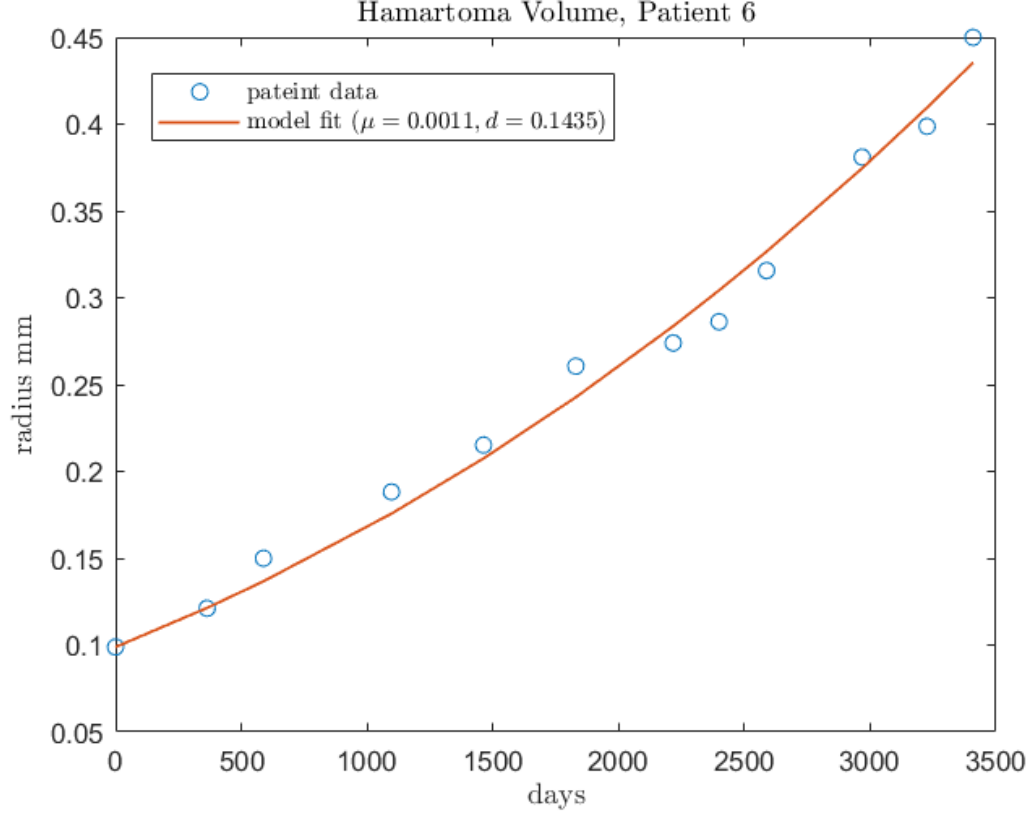


Figure 8: Hamartoma Volume Patient 6.

Symbol	Description	Value (Range)	Units	Citation
V	Volume occupied per minute (non-active NK cell)	$61.575 \cdot 10^{-9}$	$\text{mm}^3 \text{min}^{-1}$	*
V^*	Volume occupied per minute (active NK cell)	$200.120 \cdot 10^{-9}$	$\text{mm}^3 \text{min}^{-1}$	*
γ	Maximal rate of active NK cell exhaustion	$6.9 \cdot 10^{-4}$	min^{-1}	*
α_1	Rate of cytotoxic NK cell recruitment	$24 \cdot 10^{-3}$	$\text{cell mm}^{-3} \text{min}^{-1}$	*
α_2	Rate of noncytotoxic NK cell recruitment	10^{-3}	$\text{cell mm}^{-3} \text{min}^{-1}$	*
α_3	Total rate of NK cell recruitment	$25 \cdot 10^{-3}$	$\text{cell mm}^{-3} \text{min}^{-1}$	*
ξ	Killing rate of non-active NK cells		cell min^{-1}	*
ξ^*	Killing rate of active NK cells		cell min^{-1}	*
K_1	Parameter for saturation of recruitment response to tumor cells	$3.182 \cdot 10^4$	cell mm^{-3}	*
K_2	Parameter for saturation of exhaustion response to tumor cells			*
b_n	Recruitment rate of noncytotoxic NK cells	$1.265 \cdot 10^{-2}$	$\text{cell mm}^{-3} \text{min}^{-1}$	*
b_c	Recruitment rate of cytotoxic NK cells	$1.235 \cdot 10^{-2}$	$\text{cell mm}^{-3} \text{min}^{-1}$	*
β	Death rate of NK cells	$5 \cdot 10^{-5}$	min^{-1}	[38]
r	The recruitment rate of NK_c by NK_c^*	$5.59 \cdot 10^{-4}$	min^{-1}	[28]
δ	Killing rate of active NK cells	0.1	min^{-1}	[18]
δ^*	Killing rate of non-active NK cells	$(\frac{1}{240} - \frac{1}{120})$	min^{-1}	[1]
D_C	Average cell density of epithelial tumor	10^5	cell mm^{-3}	[19]
D_G	Average density of epithelial tumor	$0.3D_C$	cell mm^{-3}	**
μ	Time for breast cancer tumor volume to duplicate	$25 \cdot 1440$	min	[48]
l_{NK}	NK cell diameter	$6 \cdot 10^{-3} - 7 \cdot 10^{-3}$	mm	[20]
v_{NK}^*	Velocity of NK cells when stimulated by ligands	$5.2 \cdot 10^{-3}$	mm min^{-1}	[18]
v_{NK}	Velocity of NK cells in absence of ligands	$0.3 \cdot 10^{-3} - 1.6 \cdot 10^{-3}$	mm min^{-1}	[18]

* composite parameter, ** assumed

Table 1: Model Parameters

Description	Value	Units	Citation
Average NK cell life span	14 - 1440	min	[38]
Duration of NK cell contact under ligand stimulation	< 10	min	[18]
Average density on NK cells in tumor tissue with NK ligands	1173	cell mm^{-3}	[18]
Average density of NK cells in tumor tissue without NK ligands	301	cell mm^{-3}	[18]
NK to tumor cell ratio with ligands	$10^3 : 10^6$		[18]
NK to tumor cell ratio without ligands	$10^2 : 10^6$		[18]

Table 2: Other Values from the Literature

CHAPTER 8

DISCUSSION AND FUTURE DIRECTIONS

In this manuscript, we have constructed a simple model of breast cancer tumor growth and immune system interactions in the context of trastuzumab treatment for HER2+ breast cancer. Our model predicts the radius of small tumors increases exponentially, while that of large tumors increases approximately linearly. Exponential growth of small tumors is consistent with the definition of tumor doubling time in [37], where doubling time is expressed as $\frac{\ln(2)}{SGR}$, where SGR stands for the specific growth rate. We found a different result for the volume doubling time of a large tumor. In particular, our model predicts the rate of growth of a large tumor is less than exponential. Ouerdani et al. also observed slower growth of large tumors [45]. Indeed, [45] used ODEs to develop a combination model of growth for benign tumors in patients with neurofibromatosis type 2. The model, which was able to describe and predict tumor volume growth with and without treatment, involved a nonlinear growth function which approximated exponential growth for small tumors and linear growth for large tumors.

A unique feature of this work is that it incorporates geometric constraints into an ODE model of a tumor-immune system. Like free boundary problem models [67, 15, 7, 24], our model assumes constant tumor density and, similar to a subset of these works, our model assumes a quiescent tumor core [15]. However, our model differs in that it allows density to vary between core and growth regions. This assumption provides a distinct conservation law for tumor growth. Like our model without immune system activation, [24] concludes that tumors exhibiting fast proliferation can grow indefinitely. However, unlike our simple model, this tumor model exhibits steady states when proliferation is slow. Since growth in [24] is limited by the diffusion of nutrients, we expect that, similar to our model, proliferation will be concentrated in the outermost region of the tumor in this model. However, in [24] low nutrient concentrations can cause a net loss of cells, and this is likely the source of the model steady states.

It is interesting to compare our results on tumor-immune system interactions to those in [17] where a fractional kill rate was used for CD8⁺ T cell killing and a mass action kill rate was used for NK cell killing. In this work, the functional forms of

the kill rate were chosen to efficiently fit data. However, the most efficient model is not necessarily well-suited for describing all scenarios and different functional forms may be indistinguishable in their ability to describe some data. For example, the mechanistic model of NK cell killing developed here takes a fractional form, which approximates a mass action rate when $\delta \gg VD_G$. While [17] concluded that T cells were essential for tumor control, this work suggests that trastuzumab-induced activation of NK cells can be sufficient for HER2+ breast cancer tumor control in some patients. In particular, in patients with sufficiently high levels of patrolling NK cells or in those with sufficient activation-induced NK cells proliferation, trastuzumab treatment is predicted to eliminate tumors. In patients with weaker immune systems, the outcome of trastuzumab treatment is predicted to depend heavily on the aggressiveness of the tumor, specifically, on the tumor proliferation rate and tumor cell density. Future work will delineate regions of concern in terms of patient- and cancer-associated parameters.

It should be noted that our spatial model of tumor growth and with immune cell interactions has many limitations. For example, the model assumes a spherical tumor where the tissue is homogeneous within each region, and it does not account for the possibility of net loss of cells resulting from the death of cells in the tumor core. Since some therapies can penetrate the cellular matrix to target tumor cells within the core [55], as a future work, we are developing a more complex model that accounts for net loss as a result of cell death in the tumor interior.

CHAPTER 9

CONCLUSION

We have constructed a simple mechanistic model of tumor growth with and without drug-induced immune system activation. The model is mathematically tractable and able to reproduce a variety of growth types and patient tumor volume data. In particular, the model fit hamartoma data well, and parameter estimation suggests this data spans exponential and sub-exponential growth regimes. We have also developed a model for NK cell dynamics within breast cancer tissue, which includes a mechanistic model of NK cell activation and killing in the context of trastuzumab treatment of HER2+ breast cancer. This model predicts that we cannot control aggressive tumors exhibiting very fast proliferation or high tumor cell density by increasing NK cell cytotoxicity. However, increasing the density of patrolling NK cells or proliferation of activated NK cells leads to robust tumor control.

BIBLIOGRAPHY

References

- [1] Galit Alter, Jessica M Malenfant, and Marcus Altfeld. CD107a as a functional marker for the identification of natural killer cell activity. *Journal of immunological methods*, 294(1-2):15–22, 2004.
- [2] José Baselga, Xavier Carbonell, Noel-Jaime Castañeda-Soto, Michael Clemens, Michael Green, Vernon Harvey, Serafin Morales, Claire Barton, and Parviz Ghahramani. Phase ii study of efficacy, safety, and pharmacokinetics of trastuzumab monotherapy administered on a 3-weekly schedule. *Journal of Clinical Oncology*, 23(10):2162–2171, 2005.
- [3] Sebastien Benzekry, Clare Lamont, Dominique Barbolosi, Lynn Hlatky, and Philip Hahnfeldt. Mathematical modeling of tumor–tumor distant interactions supports a systemic control of tumor growth. *Cancer research*, 77(18):5183–5193, 2017.
- [4] Valentina Bonanni, Giuseppe Sciumè, Angela Santoni, and Giovanni Bernardini. Bone marrow NK cells: Origin, distinctive features, and requirements for tissue localization. *Frontiers in Immunology*, 10:1569, 2019.
- [5] Breastcancer.org. How chemotherapy affects the immune system.
- [6] Rene Bruno, Carla B Washington, Jian-Feng Lu, Grazyna Lieberman, Ludger Banken, and Pamela Klein. Population pharmacokinetics of trastuzumab in patients with HER2+ metastatic breast cancer. *Cancer chemotherapy and pharmacology*, 56:361–369, 2005.
- [7] HM Byrne and M A_ J Chaplain. Growth of nonnecrotic tumors in the presence and absence of inhibitors. *Mathematical biosciences*, 130(2):151–181, 1995.
- [8] Paolo Carrega, Irene Bonaccorsi, Emma Di Carlo, Barbara Morandi, Petra Paul, Valeria Rizzello, Giuseppe Cipollone, Giuseppe Navarra, Maria Cristina Mingari, Lorenzo Moretta, et al. CD56(bright)perforin(low) noncytotoxic human NK cells are abundant in both healthy and neoplastic solid tissues and

- recirculate to secondary lymphoid organs via afferent lymph. *The Journal of Immunology*, 192(8):3805–3815, 2014.
- [9] Isaac S Chan, Hildur Knútsdóttir, Gayathri Ramakrishnan, Veena Padmanaban, Manisha Warriar, Juan Carlos Ramirez, Matthew Dunworth, Hao Zhang, Elizabeth M Jaffee, Joel S Bader, et al. Cancer cells educate natural killer cells to a metastasis-promoting cell state. *Journal of Cell Biology*, 219(9), 2020.
- [10] Kevin J Cheung, Edward Gabrielson, Zena Werb, and Andrew J Ewald. Collective invasion in breast cancer requires a conserved basal epithelial program. *Cell*, 155(7):1639–1651, 2013.
- [11] Kevin J Cheung, Veena Padmanaban, Vanesa Silvestri, Koen Schipper, Joshua D Cohen, Amanda N Fairchild, Michael A Gorin, James E Verdone, Kenneth J Pienta, Joel S Bader, et al. Polyclonal breast cancer metastases arise from collective dissemination of keratin 14-expressing tumor cell clusters. *Proceedings of the National Academy of Sciences*, 113(7):E854–E863, 2016.
- [12] Jessica L Christenson, Kiel T Butterfield, Nicole S Spoelstra, John D Norris, Jatinder S Josan, Julie A Pollock, Donald P McDonnell, Benita S Katzenellenbogen, John A Katzenellenbogen, and Jennifer K Richer. MMTV-PyMT and derived Met-1 mouse mammary tumor cells as models for studying the role of the androgen receptor in triple-negative breast cancer progression. *Hormones and Cancer*, 8:69–77, 2017.
- [13] Laurent Claret, Pascal Girard, Paulo M Hoff, Eric Van Cutsem, Klaas P Zuideweld, Karin Jorga, Jan Fagerberg, and René Bruno. Model-based prediction of phase III overall survival in colorectal cancer on the basis of phase II tumor dynamics. *Journal of Clinical Oncology*, 27(25):4103–4108, 2009.
- [14] Andrew J Coldman and JM Murray. Optimal control for a stochastic model of cancer chemotherapy. *Mathematical biosciences*, 168(2):187–200, 2000.
- [15] Shangbin Cui. Asymptotic stability of the stationary solution for a parabolic-hyperbolic free boundary problem modeling tumor growth. *SIAM Journal on Mathematical Analysis*, 45(5):2870–2893, 2013.

- [16] Lisette G De Pillis and Ami Radunskaya. A mathematical tumor model with immune resistance and drug therapy: an optimal control approach. *Computational and Mathematical Methods in Medicine*, 3(2):79–100, 2001.
- [17] Lisette G de Pillis, Ami E Radunskaya, and Charles L Wiseman. A validated mathematical model of cell-mediated immune response to tumor growth. *Cancer research*, 65(17):7950–7958, 2005.
- [18] Jacques Deguine, Béatrice Breart, Fabrice Lemaître, James P Di Santo, and Philippe Bousso. Intravital imaging reveals distinct dynamics for natural killer and CD8+ T cells during tumor regression. *Immunity*, 33(4):632–644, 2010.
- [19] Ugo Del Monte. Does the cell number 10^9 still really fit one gram of tumor tissue? *Cell cycle*, 8(3):505–506, 2009.
- [20] Alexandra J Dickinson, Megan Meyer, Erica A Pawlak, Shawn Gomez, Ilona Jaspers, and Nancy L Allbritton. Analysis of sphingosine kinase activity in single natural killer cells from peripheral blood. *Integrative Biology*, 7(4):392–401, 2015.
- [21] Eurofins. Methods to determine the binding of trastuzumab to HER2. *Bioanalytical Services*, 2014.
- [22] Centers for Disease Control and Prevention. An Update on Cancer Deaths in the United States.
- [23] Miriam Franklin, Emma Connolly, and Tracy Hussell. Recruited and Tissue-Resident Natural Killer Cells in the Lung During Infection and Cancer. *Frontiers in Immunology*, page 2921, 2022.
- [24] Avner Friedman and King-Yeung Lam. Analysis of a free-boundary tumor model with angiogenesis. *Journal of Differential Equations*, 259(12):7636–7661, 2015.
- [25] Hiroyuki Fujisaki, Harumi Kakuda, Noriko Shimasaki, Chihaya Imai, Jing Ma, Timothy Lockey, Paul Eldridge, Wing H Leung, and Dario Campana. Expansion of highly cytotoxic human natural killer cells for cancer cell therapy. *Cancer research*, 69(9):4010–4017, 2009.

- [26] Kym R Garrod, Sindy H Wei, Ian Parker, and Michael D Cahalan. Natural killer cells actively patrol peripheral lymph nodes forming stable conjugates to eliminate MHC-mismatched targets. *Proceedings of the National Academy of Sciences*, 104(29):12081–12086, 2007.
- [27] Sandhya Girish, Manish Gupta, Bei Wang, Dan Lu, Ian E Krop, Charles L Vogel, Howard A Burriss III, Patricia M LoRusso, Joo-Hee Yi, Ola Saad, et al. Clinical pharmacology of trastuzumab emtansine (T-DM1): an antibody–drug conjugate in development for the treatment of HER2-positive cancer. *Cancer chemotherapy and pharmacology*, 69:1229–1240, 2012.
- [28] Rickard Glas, Lars Franksson, Clas Une, Maija-Leena Eloranta, Claes Öhlén, Anders Örn, and Klas Kärre. Recruitment and activation of natural killer (NK) cells in vivo determined by the target cell phenotype: an adaptive component of NK cell–mediated responses. *The Journal of experimental medicine*, 191(1):129–138, 2000.
- [29] Wenrui Hao, Jonathan D Hauenstein, Bei Hu, Yuan Liu, Andrew J Somnese, and Yong-Tao Zhang. Continuation along bifurcation branches for a tumor model with a necrotic core. *Journal of Scientific Computing*, 53:395–413, 2012.
- [30] Wenhua He, Ruixiang Xing, and Bei Hu. The linear stability for a free boundary problem modeling multilayer tumor growth with time delay. *Mathematical Methods in the Applied Sciences*, 45(11):7096–7118, 2022.
- [31] National Cancer Institute. Cancer stat facts: Common cancer sites.
- [32] National Cancer Institute. Funding for research areas.
- [33] Anahid Jewett and Benjamin Bonavida. Target-induced inactivation and cell death by apoptosis in a subset of human NK cells. *Journal of immunology (Baltimore, Md.: 1950)*, 156(3):907–915, 1996.
- [34] Natalie Kronik, Yuri Kogan, Moran Elishmereni, Karin Halevi-Tobias, Stanimir Vuk-Pavlović, and Zvia Agur. Predicting outcomes of prostate cancer immunotherapy by personalized mathematical models. *PloS one*, 5(12):e15482, 2010.

- [35] Lewis L Lanier, Joyce J Ruitenberg, and JH Phillips. Functional and biochemical analysis of CD16 antigen on natural killer cells and granulocytes. *Journal of immunology (Baltimore, Md.: 1950)*, 141(10):3478–3485, 1988.
- [36] Jan Lankelma, Rafael Fernández Luque, Henk Dekker, Wim Schinkel, and Herbert M Pinedo. A mathematical model of drug transport in human breast cancer. *Microvascular research*, 59(1):149–161, 2000.
- [37] Su Hyun Lee, Young-Seon Kim, Wonshik Han, Han Suk Ryu, Jung Min Chang, Nariya Cho, and Woo Kyung Moon. Tumor growth rate of invasive breast cancers during wait times for surgery assessed by ultrasonography. *Medicine*, 95(37), 2016.
- [38] Lacy E Lowry and William A Zehring. Potentiation of natural killer cells for cancer immunotherapy: a review of literature. *Frontiers in immunology*, 8:1061, 2017.
- [39] Mahmoud BA Mansour and Asmaa H Abobakr. Stochastic differential equation models for tumor population growth. *Chaos, Solitons & Fractals*, 164:112738, 2022.
- [40] Gaëtan Mary, Brice Malgras, Jose Efrain Perez, Irène Nagle, Nathalie Luciani, Cynthia Pimpie, Atef Asnacios, Marc Pocard, Myriam Reffay, and Claire Wilhelm. Magnetic compression of tumor spheroids increases cell proliferation in vitro and cancer progression in vivo. *Cancers*, 14(2):366, 2022.
- [41] Syed Awab Ali; Francesk Mulita. Hamartoma.
- [42] Gabriel E Neurohr and Angelika Amon. Relevance and regulation of cell density. *Trends in cell biology*, 30(3):213–225, 2020.
- [43] Segun Isaac Oke, Maba Boniface Matadi, and Sibusiso Southwell Xulu. Optimal control analysis of a mathematical model for breast cancer. *Mathematical and Computational Applications*, 23(2):21, 2018.
- [44] World Health Organization. Cancer.
- [45] Aziz Ouerdani, Stéphane Goutagny, Michel Kalamarides, Iñaki F Trocóniz, and Benjamin Ribba. Mechanism-based modeling of the clinical effects of be-

- vacizumab and everolimus on vestibular schwannomas of patients with neurofibromatosis type 2. *Cancer chemotherapy and pharmacology*, 77:1263–1273, 2016.
- [46] Timothy E O’Sullivan, Joseph C Sun, and Lewis L Lanier. Natural killer cell memory. *Immunity*, 43(4):634–645, 2015.
- [47] Aena Patel, Nisha Unni, and Yan Peng. The changing paradigm for the treatment of HER2-positive breast cancer. *Cancers*, 12(8):2081, 2020.
- [48] Alexander W Pearlman. Breast cancer—influence of growth rate on prognosis and treatment evaluation. a study based on mastectomy scar recurrences. *Cancer*, 38(4):1826–1833, 1976.
- [49] Víctor M Pérez-García, Gabriel F Calvo, Jesús J Bosque, Odelaisy León-Triana, Juan Jiménez, Julián Pérez-Beteta, Juan Belmonte-Beitia, Manuel Valiente, Lucía Zhu, Pedro García-Gómez, et al. Universal scaling laws rule explosive growth in human cancers. *Nature physics*, 16(12):1232–1237, 2020.
- [50] Guang He Ran, Yu Qing Lin, Lei Tian, Tao Zhang, Dong Mei Yan, Jian Hua Yu, and You Cai Deng. Natural killer cell homing and trafficking in tissues and tumors: from biology to application. *Signal Transduction and Targeted Therapy*, 7(1):205, 2022.
- [51] Benjamin Ribba, Gentian Kaloshi, Mathieu Peyre, Damien Ricard, Vincent Calvez, Michel Tod, Branka Čajavec-Bernard, Ahmed Idbah, Dimitri Psimaras, Linda Dainese, et al. A tumor growth inhibition model for low-grade glioma treated with chemotherapy or radiotherapy. *Clinical Cancer Research*, 18(18):5071–5080, 2012.
- [52] George Scaria, Trevor Argall, Laura Bendzick, and Dan S Kaufman. Increased telomere length in natural killer cells generated from human induced pluripotent stem cells. *Blood*, 124(21):5816, 2014.
- [53] American Cancer Society. Breast Cancer HER2 status.
- [54] James Stewart, Daniel K Clegg, and Saleem Watson. *Calculus: early transcendentals*. Cengage Learning, 2020.

- [55] Árpád Szöőr, Gábor Tóth, Barbara Zsebik, Viktória Szabó, Zelig Eshhar, Hinrich Abken, and György Vereb. Trastuzumab derived HER2-specific CARs for the treatment of trastuzumab-resistant breast cancer: CAR T cells penetrate and eradicate tumors that are not accessible to antibodies. *Cancer Letters*, 484:1–8, 2020.
- [56] Gerald Teschl. *Ordinary differential equations and dynamical systems*, volume 140. American Mathematical Soc., 2012.
- [57] Nicola J Topham and Eric W Hewitt. Natural killer cell cytotoxicity: how do they pull the trigger? *Immunology*, 128(1):7–15, 2009.
- [58] Marc Turini, Patrick Chames, Pierre Bruhns, Daniel Baty, and Brigitte Kerfelec. A Fc γ riii-engaging bispecific antibody expands the range of HER2-expressing breast tumors eligible to antibody therapy. *Oncotarget*, 5(14):5304, 2014.
- [59] Sébastien Viel, Emily Charrier, Antoine Marçais, Paul Rouzair, Jacques Bienvenu, Lionel Karlin, Gilles Salles, and Thierry Walzer. Monitoring NK cell activity in patients with hematological malignancies. *Oncoimmunology*, 2(9):e26011, 2013.
- [60] Shuo Wang and Heinz Schättler. Optimal control of a mathematical model for cancer chemotherapy under tumor heterogeneity. *Mathematical Biosciences and Engineering*, 13(6):1223–1240, 2016.
- [61] Yoichi Watanabe, Erik L Dahlman, Kevin Z Leder, and Susanta K Hui. A mathematical model of tumor growth and its response to single irradiation. *Theoretical Biology and Medical Modelling*, 13:1–20, 2016.
- [62] Jared A Weis, Michael I Miga, Lori R Arlinghaus, Xia Li, Vandana Abramson, A Bapsi Chakravarthy, Praveen Pendyala, and Thomas E Yankeelov. Predicting the response of breast cancer to neoadjuvant therapy using a mechanically coupled reaction–diffusion modelbiomechanical model for predicting breast cancer response. *Cancer research*, 75(22):4697–4707, 2015.
- [63] Jared A Weis, Michael I Miga, Lori R Arlinghaus, Xia Li, A Bapsi Chakravarthy, Vandana Abramson, Jaime Farley, and Thomas E Yankeelov.

- A mechanically coupled reaction–diffusion model for predicting the response of breast tumors to neoadjuvant chemotherapy. *Physics in Medicine & Biology*, 58(17):5851, 2013.
- [64] Sherry X Yang, Stephen M Hewitt, and John Yu. Locoregional tumor burden and risk of mortality in metastatic breast cancer. *NPJ Precision Oncology*, 6(1):22, 2022.
- [65] Anyue Yin, Dirk Jan AR Moes, Johan GC van Hasselt, Jesse J Swen, and Henk-Jan Guchelaar. A review of mathematical models for tumor dynamics and treatment resistance evolution of solid tumors. *CPT: pharmacometrics & systems pharmacology*, 8(10):720–737, 2019.
- [66] Guoxu Zheng, Zhangyan Guo, Weimiao Li, Wenjin Xi, Baile Zuo, Rui Zhang, Weihong Wen, An-Gang Yang, and Lintao Jia. Interaction between HLA-G and NK cell receptor KIR2DL4. orchestrates HER2-positive breast cancer resistance to trastuzumab. *Signal Transduction and Targeted Therapy*, 6(1):236, 2021.
- [67] Jiayue Zheng and Shangbin Cui. Analysis of a tumor model free boundary problem with action of an inhibitor and nonlinear boundary conditions. *Journal of Mathematical Analysis and Applications*, 496(1):124793, 2021.
- [68] Huang Zhu, Robert H Blum, Ryan Bjordahl, Svetlana Gaidarova, Paul Rogers, Tom Tong Lee, Ramzey Abujarour, Gregory B Bonello, Jianming Wu, Pei-Fang Tsai, et al. Pluripotent stem cell-derived NK cells with high-affinity noncleavable CD16a mediate improved antitumor activity. *Blood*, 135(6):399–410, 2020.